Spatial and temporal variations of precipitation during 1979–2015 in Jinan City, China

Xiaodong Chang, Zongxue Xu, Gang Zhao, Tao Cheng and Sulin Song

ABSTRACT

The spatiotemporal variation of precipitation significantly affects regional hydrological processes and the management of water resources worldwide, indirectly contributing to an aggravation in the frequency and intensity of extreme events, especially in urban areas. To analyze the spatiotemporal variation characteristics of precipitation during 1979–2015 in Jinan City, the China Meteorological Forcing Dataset and 12 precipitation-related indices are adopted and analyzed by using Mann–Kendall trend test, Sen's slope estimator and Pettitt test in this study. The results show that: (1) the annual mean precipitation (AMP) shows a gradual increasing trend from the northern plain area to the southern mountainous area; (2) the heaviest summer precipitation occurs in the southern part of downtown with a high frequency, resulting in the drastic amplification of urban rainstorm flood disasters; (3) the spatial distributions of most indices show a gradual increasing trend from the northern plain area to the southern mountainous area, while consecutive dry days show the opposite tendency; and (4) most indices roughly show similar spatiotemporal variation characteristics with AMP, i.e., decreases in southwestern area, but increases in the eastern mountainous region and the north plain area, exhibiting an overall increasing trend at the 1% significance level.

Key words | Jinan City, precipitation, spatiotemporal variation

Xiaodong Chang
Zongxue Xu (corresponding author)
Gang Zhao
Tao Cheng
College of Water Sciences,
Beijing Normal University,
Beijing 100875,
China
E-mail: *zongxuexu@vip.sina.com*

Sulin Song
Jinan Hydrology Bureau,
Jinan 250014,
China

INTRODUCTION

With the intensification of global warming and extreme climatic events, growing concern about global and regional climate change has been attracting broad attention over the past few decades (Hansen *et al.* 2016). According to the Fifth Assessment Report of the IPCC, the annual precipitation has increased significantly over the northern hemisphere since 1951, especially for the mid-latitude land areas (high confidence), but area-averaged long-term positive or negative trends have low confidence for other latitudes, which has had a strong and comprehensive impact on the global hydrological cycle (IPCC 2014). Anthropogenic forcing has also made a substantial contribution to changes in precipitation over most regions in the last century. Along with the rapid economic and social development, the rain island effect and tropical island effect induced by continuous urban expansion have become more serious, causing a continuous increase in precipitation over most urban and suburban areas in China (Jauregui & Romales 1996; Xu *et al.* 2010). Also, it has been well acknowledged that regional and local extreme precipitation changes, especially the changes in frequency, intensity, and amount of heavy precipitation that trigger frequent meteorological disasters, such as rainstorms and flash floods, are more likely to cause catastrophic consequences (Bonsal *et al.* 2001; Liu *et al.* 2013). As an important meteorological and hydrological element, precipitation varies greatly over its spatial and temporal distribution (Xu *et al.* 2005). To reduce these relevant impacts and assess the

doi: 10.2166/wcc.2017.029

potential risks for the management of water resources, the detection and attribution of variation in precipitation characteristics play an important role in decision-making when considering, for example, societal adaptation to future regional and local changes in precipitation (Madsen *et al.* 2014; Xu & Chu 2015).

During the past few decades, research regarding the spatiotemporal variations of precipitation mainly based on the Mann–Kendall (M–K) trend test has received a great deal of attention in many regions, such as Spain, Canada, and the Nepal Himalayas (Esteban-Parra *et al.* 1998; Bonsal *et al.* 2001; Panthi *et al.* 2015). Furthermore, multiple studies have suggested that different regions in China have experienced various change patterns: the annual mean precipitation (AMP) of northeast China, middle and lower Yellow River Basin, middle and upper Pearl River Basin is dominated by a decreasing trend, especially after 1970, while in southeast China and the middle and lower Yangtze River Basin, it is dominated by a significant increase of the amount and intensity (Liu *et al.* 2008; Zhang *et al.* 2008, 2009, 2012; Jianting *et al.* 2010). As above, most of the current studies are focused on a macroscale variation analysis of meteorological and hydrological characteristics. However, for rapidly urbanized regions with a relatively smaller scale and higher exposure and vulnerability to drought, flood and waterlogging disasters, spatiotemporal variation analysis of precipitation, especially for extreme precipitation that usually causes enormous economic losses and mass casualties, is also very necessary there. During the last few decades, relevant research has been limited by the accessibility of a long-term meteorological station database and the site distribution density. However, the emergence of a high resolution assimilation dataset has made the microscale variation analysis of meteorological and hydrological characteristics possible in urban areas with insufficient observed data in recent years (Xu & Chu 2015; Hansen *et al.* 2016).

Located in the north of the capital economic circle and south of the Yangtze River Delta economic area, Jinan lies in the middle and lower reaches of the Yellow River Basin, which plays an important role in the economic development and ecological civilization construction of China. Due to the influence of the warm temperate monsoon climate and great variation in topography, the spatiotemporal distribution of precipitation in Jinan City is extremely uneven, with more than 60% of the annual total precipitation concentrated from June to September, resulting in summer being the main flooding season. Meanwhile, the dramatic change of Jinan's urban form and environmental landscape leads to the regional economic society showing high sensitivity to extreme precipitation. Natural precipitation-related hazards, such as severe agricultural droughts and frequent flood waterlogging disasters, have caused enormous economic losses and thus hindered socioeconomic development there. Although the regional characteristics of precipitation are significant, few studies regarding spatial and temporal variation analysis with high resolution datasets have been performed so far, not to mention the variation tendency of recent years in Jinan City. Thus, it is urgent to conduct a study of the surface precipitation characteristics during recent years in Jinan City.

As a typical piedmont city, further study of the precipitation distribution and variation characteristics based on the long-term sequenced and high-resolution meteorological dataset has great theoretical and practical significance. Therefore, the major objectives of this study were to detect and quantitatively analyze the spatial distribution characteristics and the spatiotemporal variation tendency of precipitation based on the high-resolution assimilated datasets in Jinan and to investigate the correlations of the 12 selected precipitation-related indices. A further understanding and detailed analysis of the precipitation variation characteristics may also help to reduce climate-induced drought–flood disasters and provide a useful reference for water resource management in Jinan City.

MATERIALS AND METHODS

Study area description

Located downstream of the Yellow River and north of Mount Tai, Jinan City is the political, economic, cultural, scientific and technological center of Shandong Province in China, with a total population of more than seven million in 2015. Ranging from 36°10′N to 37°40′N and 116°12′E to 117°44′E, Jinan City covers an area of approximately

8,117 km^2, with a main urban area of 525 km^2, and the terrain slopes downward gradually from the southeast to the northwest (Figure 1(a) and 1(b)). Based on the administrative boundary and UNEP-WCMC standard (Tang *et al.* 2006), Jinan City is primarily divided into three topographic regions, namely, the mountainous area, plain area, and urban area (Figure 1(c)).

As a zone of the mid-latitude northern hemisphere, the regional climate is a temperate continental monsoon climate, where the temperature difference in summers and winters is obvious. The mean annual precipitation is approximately 636 mm, and the average annual temperature is 14.7° C, which is characterized by abundant precipitation and high temperatures from June to August. Affected by the intensity of monsoon and a cycle of interannual variation, the regional rainfall changes correspondingly, which means that rainfall will increase in strong summer monsoon years, and vice versa.

The rivers in Jinan City belong to the Yellow River system and the Xiaoqinghe River system, and most tributaries are seasonal streams during flood seasons, which mainly depend on rainfall recharge as the source of water. In addition, the uneven spatial distribution of precipitation makes a clear distinction between the flood period and dry period within a year. On the one hand, Jinan belongs to a geographically complicated hilly and mountainous area. On the other hand, its flood season is mainly concentrated in July and August each year, usually accounting for over 65% of the total annual precipitation, thus resulting in the exacerbation of flood risk in the main urban area of Jinan City (Cui *et al.* 2009).

Data analysis

The China Meteorological Forcing Dataset (CMFD) was employed in this study, which was developed by the Institute of Tibetan Plateau Research in the Chinese Academy of Sciences and includes seven meteorological elements, namely, temperature, precipitation, pressure, specific humidity, wind speed, and downward shortwave and longwave radiation, covering the period from 1 January 1979 to 31 December 2015 (Chen *et al.* 2011; and http://westdc.westgis.ac.cn/data/7a35329c-c53f-4267-aa07-e0037d913a21). The meteorological dataset took TRMM (Tropical Rainfall Measuring Mission) satellite precipitation analysis data (3B42), GEWEX-SRB (Global Energy and Water Cycle Experiment – Surface Radiation Budget) downward shortwave radiation data, Princeton forcing data and GLDAS data as the climatological background field, and the observed CMA (China Meteorological Administration) station data are interpolated to grid points, with a spatial resolution of 0.1° and temporal resolution of 3 hr (Jie & Kun 2011).

Simple quality control was first carried out to ensure that the precipitation data were reasonable by eliminating data values exceeding 3 standard deviations from the mean. Field observations of precipitation data, most covering the period from 1977 to 2014, were also collected from several local hydrological stations provided by the Jinan Hydrographic Office for data verification.

Due to the lack of hydrological stations with long sequences of meteorological data in Jinan City, four

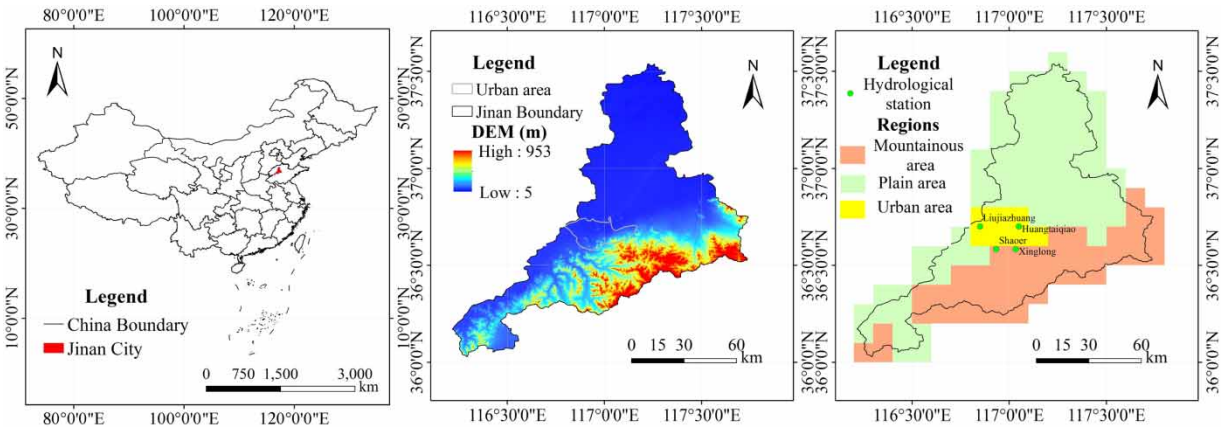

Figure 1 | (a) Geographic location of Jinan City in China; (b) digital elevation map of Jinan City and its main urban area; and (c) topographical division of Jinan City.

hydrological stations (see Figure 1(c)) with observed precipitation data in the main flood season (i.e., May to October) around the main urban area were selected as a comparison, and the verification period ranges from 1979 to 2014 which ensures the consistency of the observed and CMFD data. The mean annual precipitation in the main flood season (M1), mean annual maximum 1-day precipitation in the main flood season (M2), and mean annual count of days in the main flood season when daily precipitation ≥20 mm (M3) were adopted to verify the accuracy and reliability of CMFD (Table 1). According to Table 1, the overwhelming majority of relative errors are within 20%, except for M3 in Huangtaiqiao station, which means that the CMFD is accurate and reliable in this study.

Methods description

In this study, the temporal trends and spatial distributions of precipitation-related indices in Jinan City during 1979–2015 are examined by the M–K trend test and calculated by Sen's slope estimator. Abrupt change points in an observed time series of precipitation are detected by the Pettitt test. The principles of calculating the indices and methods are described in detail as follows.

Precipitation indices

The World Meteorological Organization (WMO) Expert Team on Climate Change Detection and Indices (ETCCDI) recommended 27 core extreme indices that provided a comprehensive overview of extreme temperature and precipitation, which had relatively weak extremes, low noise and strong significances that reflect the change of extreme climate in different aspects and thus have multiple applications in climate research and related fields (Sillmann *et al.* 2013; Wang & Li 2016). In this case, 12 extreme precipitation-related indices were selected and modified correspondingly to reflect the local situation in this study, as shown in Table 2.

M–K trend test

The non-parametric M–K statistical test (Mann 1945; Kendall 1975), which is a rank-based procedure, is frequently applied to characterize the trends in climate data series (Xu & Chu 2015). In this study, the M–K test is used to analyze the trends for precipitation-related indices and to test their significance.

In the M–K test, the test statistic is calculated as follows:

$$S = \sum_{i=1}^{n-1} \sum_{j=i+1}^{n} \operatorname{sgn}(x_j - x_i) \tag{1}$$

where

$$\operatorname{sgn}(x_j - x_i) = \begin{cases} +1, x_j > x_i \\ 0, x_j = x_i \\ -1, x_j < x_i \end{cases} \tag{2}$$

In Equations (1) and (2), x_j and x_i are the sequential data values and n is the number of data points. The statistic S is approximately normally distributed when $n \geq 8$, with the mean and the variance determined by formula (Equations (3) and (4)):

$$\mathrm{E}(S) = 0 \tag{3}$$

$$\mathrm{V}(S) = \frac{n(n-1)(2n+5) - \sum_{i=1}^{n} t_i i(i-1)(2t+5)}{18} \tag{4}$$

In Equation (4), n is the number of data points and t_i is the number of ties of extent i. The standard normal test

Table 1 | Data verification of CMFD and the observed dataset during 1979–2014

	Liujiazhuang station			Huangtaiqiao station			Shaoer station			Xinglong station		
Indices	Observed data	CMFD	Relative error	Observed data	CMFD	Relative error	Observed data	CMFD	Relative error	Observed data	CMFD	Relative error
M1 (mm)	465.3	421.4	−9.4%	531.1	548.2	3.2%	533.9	598.7	12.1%	544.3	640.6	17.7%
M2 (mm)	86.9	70.7	−18.6%	90.8	76.3	−16.0%	81.5	71.7	−12.0%	85.4	74.8	−12.4%
M3 (days)	7.6	7.8	2.6%	8.0	10.0	24.2%	8.7	9.8	12.5%	9.3	10.0	7.6%

Table 2 | Definitions of the 12 selected extreme precipitation indices

Indices	Description	Units
AMP	Annual mean precipitation on wet days	mm
SDII	Annual total precipitation divided by the number of wet days in the year	mm/day
Rx1day	Annual maximum 1-day precipitation	mm
Rx5day	Annual maximum consecutive 5-day precipitation	mm
R95pTOT	Annual precipitation due to very wet days when daily precipitation >95th percentile of 1979–2015 daily rainfall	mm
R99pTOT	Annual precipitation due to very wet days when daily precipitation >99th percentile of 1979–2015 daily rainfall	mm
APD	Annual count of precipitation days when daily precipitation ≥1 mm	days
R10 mm	Annual count of days when daily precipitation ≥10 mm	days
R20 mm	Annual count of days when daily precipitation ≥20 mm	days
R50 mm	Annual count of days when daily precipitation ≥50 mm	days
CDD	Maximum number of consecutive days with daily precipitation <1 mm	days
CWD	Maximum number of consecutive days with daily precipitation ≥1 mm	days

statistic Z is computed by using Equation (5):

$$Z = \begin{cases} \dfrac{s-1}{\sqrt{Var(s)}}, & S > 0 \\ 0, & S = 0 \\ \dfrac{s-1}{\sqrt{Var(s)}}, & S < 0 \end{cases} \quad (5)$$

Positive Z values indicate increasing trends, and negative Z values show decreasing trends, while zero Z values denote no change trends. The null hypothesis is rejected and a significant trend exists in the time series when $|Z| = Z_{1-\alpha/2}$, which can be obtained from the standard normal distribution table. The specific significance levels $\alpha = 0.01$ and 0.05 were adopted in this study to test trends. At the 5% significance level, the null hypothesis of no trend is rejected if $|Z| > 1.96$ and rejected if $|Z| > 2.576$ at the 1% significance level.

Furthermore, UF and UB are also set up to detect the specific variation characteristics and general change points of time series x_i. The calculation steps are as follows.

For a comparison of x_i and x_j in Equation (1), the number of cases $x_j > x_i$ are counted and denoted by r_i. Then, the test statistic S_k is:

$$S_k = \sum_{i=1}^{k} r_i \quad (k = 2, 3, \ldots, n) \quad (6)$$

The mean and variance of the test statistic are calculated as:

$$E(S_i) = \frac{i(i-1)}{4} \quad (7)$$

$$Var(S_i) = \frac{i(i-1)(2i+5)}{72} \quad (8)$$

The sequential values of the statistic UF are computed as:

$$UF = \frac{S_i - E(S_i)}{\sqrt{Var(S_i)}} \quad (i = 1, 2, \ldots, n) \quad (9)$$

Similarly, the statistic UB is computed backward from the end of the time series. If the UF and UB curves intersect and then diverge and acquire specific threshold values, then a statistically significant trend exists. In this study, a statistically significant trend of an increasing or decreasing trend is indicated if the corresponding solid line crosses over the dashed line. The point of intersection shows the approximate change point at which the trend begins.

Sen's slope estimator

At the same time, another important index, Sen's slope estimator (Sen 1968), was adopted to estimate the slope of the

trend in the sample of N pairs of data at the magnitude of the monotonic change:

$$Q_i = \frac{x_j - x_k}{j - k} \quad \text{for } j, k = 1, \ldots, N \tag{10}$$

where x_j and x_k are the data values at times j and k ($j > k$), respectively. If there is only one datum in each time period, then $N = (n(n-1)/2)$, where n is the number of time periods. If there are multiple observations in one or more time periods, then $N < (n(n-1)/2)$, where n is the total number of observations.

The N values of Q_i are ranked from smallest to largest, and the median of the slope or Sen's slope estimator is computed as:

$$Q_{med} = \begin{cases} Q_{(N+1)/2}, \text{ if } N \text{ is odd} \\ \dfrac{Q_{N/2} + Q_{(N+2)/2}}{2}, \text{ if } N \text{ is even} \end{cases} \tag{11}$$

The Q_{med} sign reflects the data trend reflection, while its value indicates the steepness of the trend. To determine whether the median slope is significantly different than zero, one should obtain the confidence interval of Q_{med} at a specific probability. The confidence interval for the time slope (Gilbert 1987) can be computed as follows:

$$C_\alpha = Z_{1-\alpha/2}\sqrt{Vas(S)} \tag{12}$$

where Var(S) is defined in Equation (3) and $Z_{1-\alpha/2}$ is obtained from the standard normal distribution table. In this study, the confidence interval was computed at two significance levels ($\alpha = 0.01$ and $\alpha = 0.05$). Then, $M_1 = ((N - C_\alpha)/2)$ and $M_2 = ((N + C_\alpha)/2)$ are computed. The lower and upper limits of the confidence interval, Q_{min} and Q_{max}, respectively, are the M_1th largest and $(M_2 + 1)$th largest of the N ordered slope estimates (Gilbert 1987). The slope Q_{med} is significantly different from zero if the two limits (Q_{min} and Q_{max}) have a similar sign.

Pettitt test

The non-parametric Pettitt test (Pettitt 1979), which detects a shift in the mean at an unknown time, has been proven to be a useful and powerful tool for detecting abrupt change points in a long-term trend analysis (Wang & Li 2016) and calculating its statistical significance; this test was selected to identify the significant change point of the time series of the precipitation dataset.

The Pettitt test considers a sequence of random variables and divides it into two groups represented by x_1; x_2;…; x_t and x_{t+1}; x_{t+2}; …; x_n. If each group has its corresponding common distribution function, then the change point is identified at t. To achieve the identification of a change point, a statistical index $U_{t,n}$ is expressed as follows:

$$U_{t,n} = \sum_{i=1}^{t}\sum_{j=t+1}^{n} \text{sgn}(x_i - x_j), \; 1 \le t \le n \tag{13}$$

where similarly,

$$sgn(x_j - x_i) = \begin{cases} +1, x_j > x_i \\ 0, x_j = x_i \\ -1, x_j < x_i \end{cases} \tag{14}$$

The most possible change point is found where its value is:

$$k_t = \max_{1 \le t \le n} |U_{t,n}| \tag{15}$$

and the significance probability associated with the value K_t is evaluated as:

$$\rho = 2\exp\left(\frac{-6k_t^2}{n^3 + n^2}\right) \tag{16}$$

If ρ is smaller than the specific significance level in Equation (16), the null hypothesis is rejected. In other words, if a significant change point exists, the time series is divided into two parts at the location of the change point t. The approximate significance probability for a change point is defined as $p = 1 - \rho$. The specific significance level is at the 95% confidence level in this study.

To understand the basic trend and variation of precipitation on the different time scales, linear fitting and five-year moving-average curves were used for the preliminary analysis of the seasonal precipitation in different regions over Jinan City during 1979–2015. In addition, Pearson correlation method was employed to analyze the temporal

variations in precipitation extremes. ArcGIS was applied to plot the spatial distributions of the variation trends for these precipitation-related indices.

RESULTS ANALYSIS AND DISCUSSION

Spatial distribution characteristics and trends of precipitation amounts in Jinan City

The AMP varies greatly in different regions from 1979 to 2015 in Jinan City. The mountainous area has the largest AMP of 797.7 mm, while the urban and plain areas are 655.6 mm and 636.3 mm, respectively. Precipitation in Jinan City varies with the season and is highest in summer, second highest in autumn, and lowest in winter. According to Figure 2, summer precipitation has the largest proportion compared with the other seasonal precipitation in all three areas, accounting for more than 60% of the total annual precipitation. Meanwhile, the heaviest summer precipitation occurs in the mountainous area, which ranged from a low of 197.7 mm in 2002 to a high of 899.0 mm in 1990, with a mean value of 494.6 mm. The spring and autumn precipitation for the whole city, which totaled approximately 15% of the total AMP, are both approximately 100 mm, while winter precipitation is the lowest, with approximately 20 mm of rainfall on average.

It is well acknowledged that alterations of wet and dry periods for each year occur over time, in which case the wet season (May to October, i.e., flood season) and dry season (November to the following April, i.e., non-flood season) were adopted based on the local precipitation characteristics.

For seasonal precipitation, wet season precipitation accounts for approximately 87.0% of the annual precipitation from 1979 to 2015. Although the mean annual precipitation shows large interannual variability, the wet season precipitation in the urban and plain areas experienced a large increase overall during this period at a rate of 19.0 mm/10 a and 29.1 mm/10 a, respectively, while it decreased at a rate of −31.0 mm/10 a in the mountainous area (Figure 3). In addition, dry season precipitation in the whole city progressively increased by a small margin. In comparison, the trend of dry season precipitation in the urban area showed little change (0.4 mm/10 a), but fluctuated over a large range, while in the plain and mountainous areas, it showed a stable increasing trend.

To further detect the statistical characteristics of precipitation in the different periods for all areas, the wet season and dry season precipitation over all of Jinan City were calculated using a M–K trend test based on the CMFD during 1979–2015.

The results obtained by the M–K method are shown by the corresponding solid lines (*UF* and *UB*), respectively, in Figure 4, and the horizontal dashed lines correspond to the confidence limits at a significance level of $\alpha = 0.05$. According to Figure 4, the variation tendency of wet season precipitation is generally consistent with that of annual precipitation in the whole city, and there is no significant trend for both the wet and dry seasons in different areas during the whole period (i.e., both are not significant at 0.05 significance level).

In concrete terms, wet season precipitation in the urban and plain areas exhibits an increasing trend for most years, which is just coincident with the trend for the surrounding four hydrological stations, but a short-term fluctuation occurs for the spring during 1979–1989 (Figure 4(a) and 4(e)), while wet season precipitation in

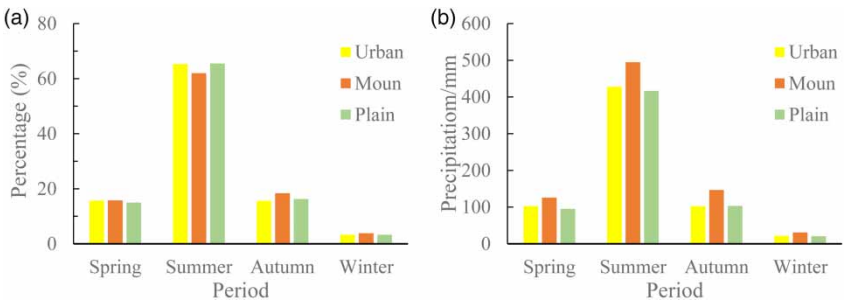

Figure 2 | (a) Contributions of seasonal precipitation to the AMP and (b) mean precipitation for different seasons over Jinan City.

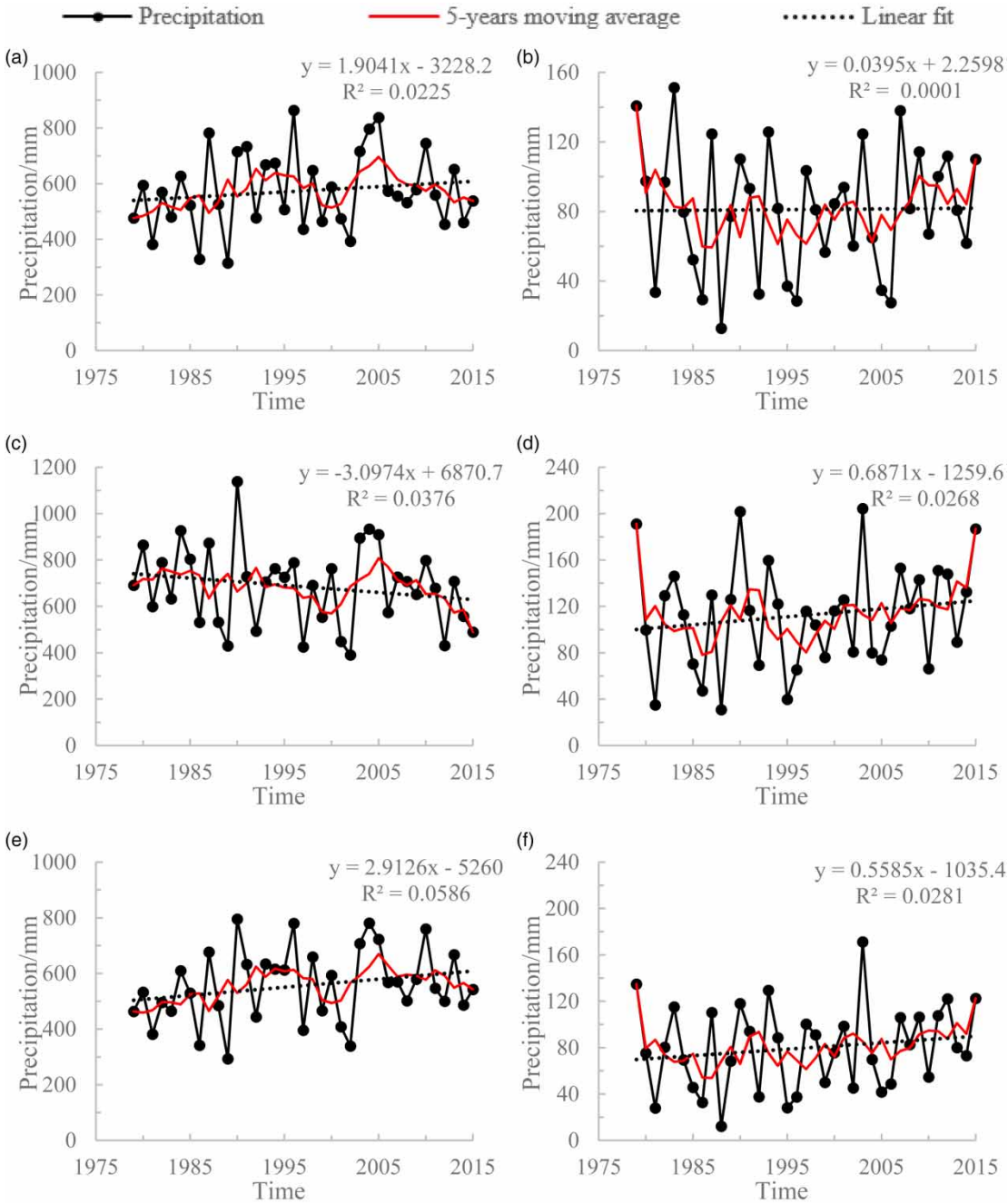

Figure 3 | Linear fitting results of precipitation from 1979 to 2015 for (a) the wet season (May to October) in the urban area, (b) the dry season (November to the following April) in the urban area, (c) the wet season in the mountainous area, (d) the dry season in the mountainous area, (e) the wet season in the plain area, and (f) the dry season in the plain area.

the mountainous area shows the exact opposite trend (Figure 4(c)). According to Figure 4(b), the dry season precipitation in the urban area decreases over the whole period. Dry season precipitation in mountainous and plain areas exhibits a declining trend in the beginning period, but both trends have increased since 2008 (Figure 4(d) and 4(f)).

In general, wet season precipitation over Jinan City shows a slowly increasing trend (statistically insignificant), while dry season precipitation declined at the end of the

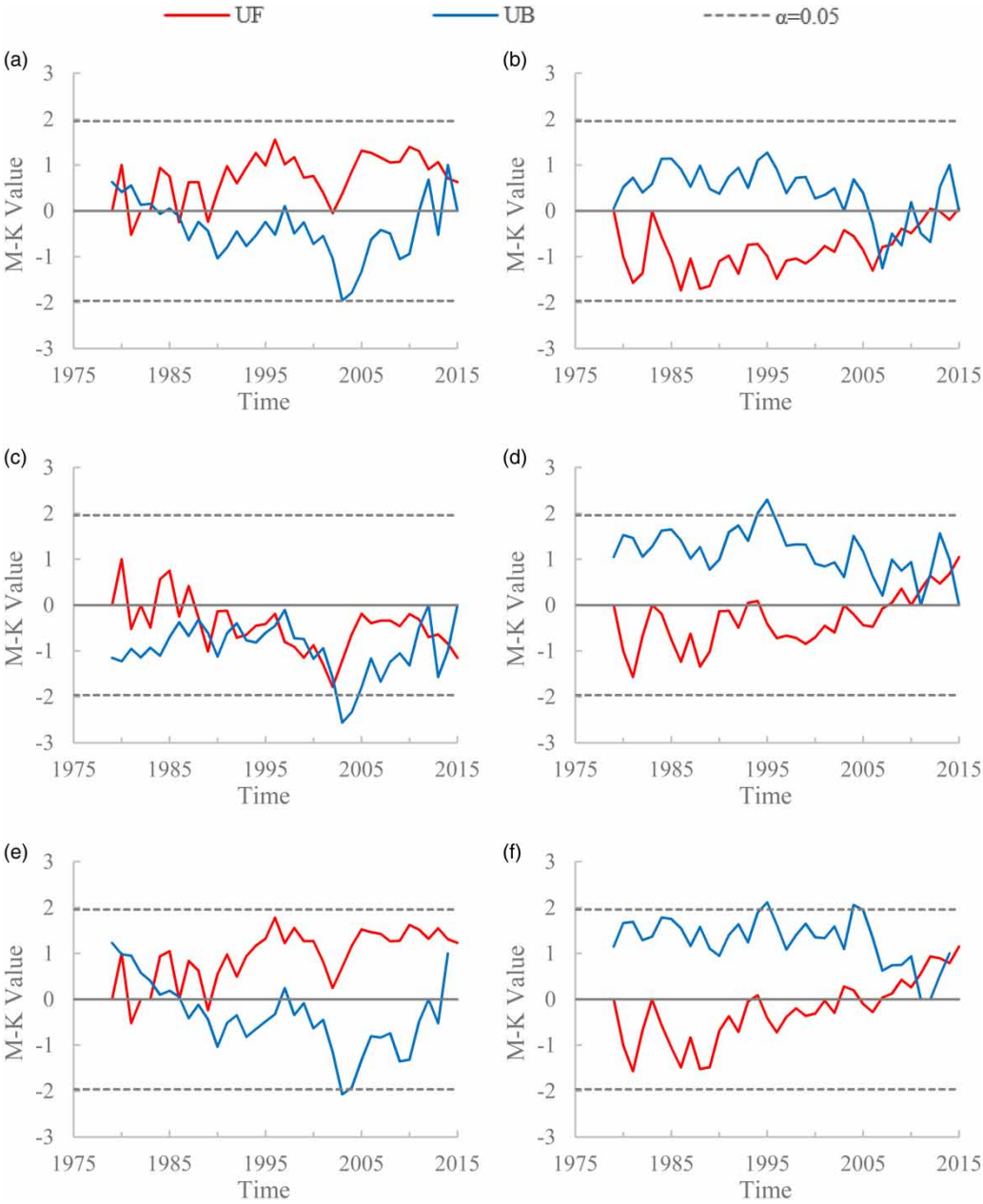

Figure 4 | The M–K test statistic results of seasonal mean precipitation from 1979 to 2015 for: (a) the wet season in the urban area, (b) the dry season in the urban area, (c) the wet season in the mountainous area, (d) the dry season in the mountainous area, (e) the wet season in the plain area, and (f) the dry season in the plain area. Dashed lines are the confidence limits at the 95% confidence level.

20th century, but increased after approximately 2005 (still statistically insignificant). Thus, there is a steadily increasing trend in the wet season that is unable to offset the remarkable decrease in the dry season, which plays a dominant role in the trends of the overall annual precipitation.

Spatial variability of 12 precipitation-related indices in Jinan City

The spatial distribution of the 12 selected precipitation indices during 1979–2015 are given in Figure 5. The mean

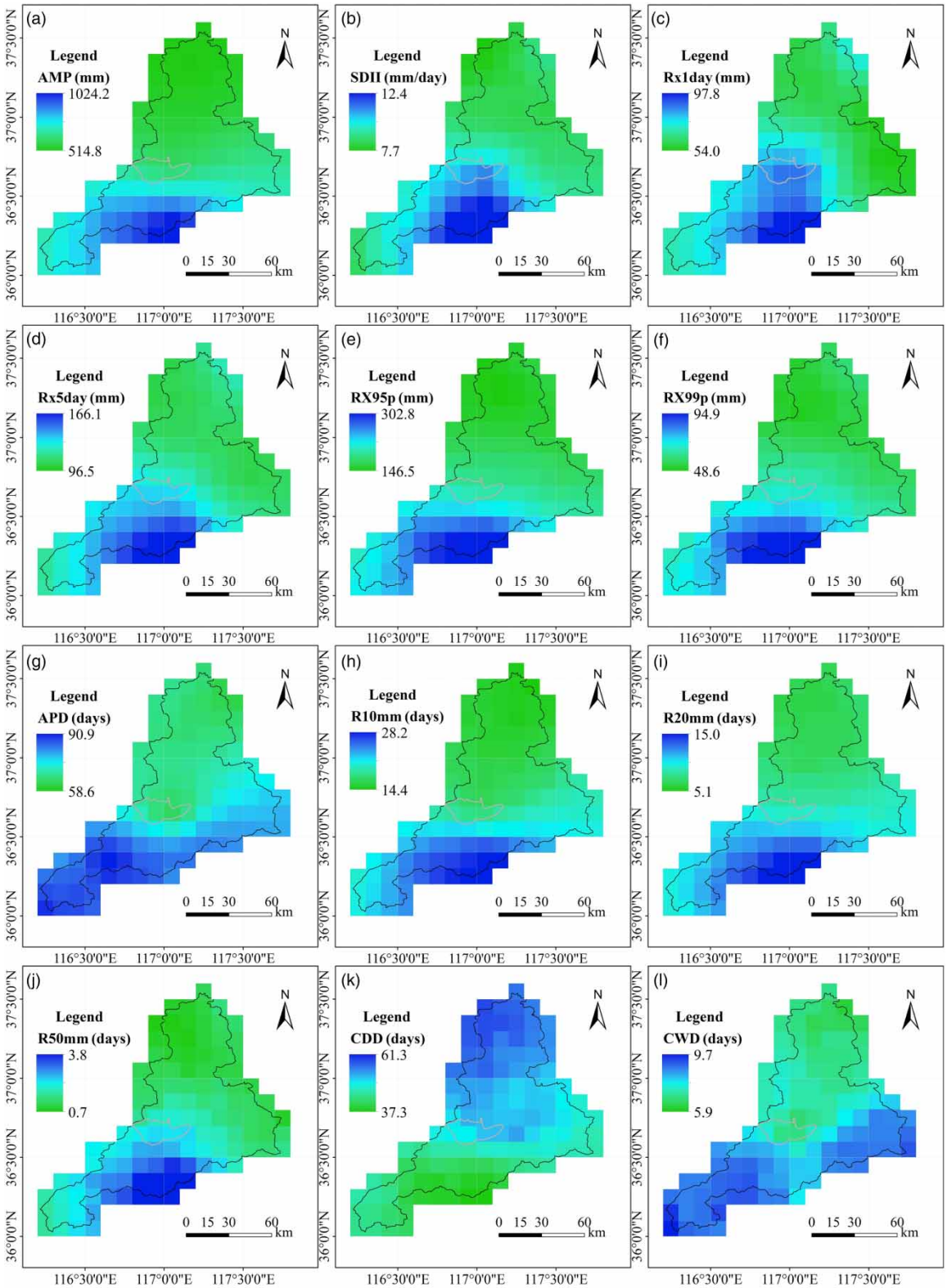

Figure 5 | Spatial variation of the 12 extreme precipitation indices from 1979 to 2015 in Jinan City. The gray line represents the boundary of the main urban area in Jinan City.

values of the 12 precipitation-related indices indicate several different spatial distribution features as follows.

First, AMP on wet days shows an increasing tendency from the northern plain to the southern mountainous area, varying from 514.8 to 1,024.2 mm, which roughly has the same spatial distribution pattern as the Yellow River Basin (Xu *et al.* 2007). Specifically, the mountainous area has the largest AMP of 797.7 mm, while it is 655.6 mm and 636.3 mm in the urban and plain areas, respectively. Meanwhile, the annual precipitation due to very wet days when the daily precipitation >95th and 99th percentile of the 1979–2015 daily rainfall (RX95p and RX99p) and the annual count of precipitation days (APD) shows the same spatial distribution characteristics as the AMP.

The annual maximum 1-day precipitation (Rx1day) and annual maximum consecutive 5-day precipitation (Rx5day) have similar spatial distribution characteristics to the AMP, but both have a gathering trend in the middle part of Jinan City, which indicates that the urban area is more likely to encounter the aggregation of rainfall events with such features as high intensities and short durations than suburban areas at similar latitudes, leading to a higher risk of floods in urban areas.

In addition, the annual count of days when the daily precipitation ≥10 and 20 mm (R10 mm and R20 mm) roughly has the same distribution characteristics as the AMP, which indicates that the distribution characteristics of light to moderate rain are consistent with those of the AMP over Jinan City. Meanwhile, the annual count of days when the daily precipitation ≥50 mm (R50 mm) has the same distribution characteristics as Rx1day, suggesting that heavy rain is much more prone to occur in the southern urban area.

The APD and maximum number of consecutive wet days (CWD) are likely concentrated on the southwestern and east mountainous areas where the AMP is not so large, indicating that these areas have less extreme precipitation. As for the maximum number of consecutive dry days (CDD), it shows a decreasing trend from the northern plain area to the southern mountainous area, varying from 37.3 to 61.3 days, which is the opposite of the AMP.

Spatiotemporal trends of 12 precipitation-related indices in Jinan City

As seen in Table 3, most of the indices over the entire Jinan City experience statistically significant increasing trends at the 0.01 significance level except for the AMP and APD. Among them, Rx1day and Rx5day display a significant increasing trend, varying from −13.3 to 13.6 and −15.2 to 24.1 mm/decade, with a regional average of 0.54 and

Table 3 | The M–K test and Pettitt test for the extreme precipitation indices over Jinan City

	M–K test				Pettitt test		
	Z value	Trends	Sen's slope	Ranges	Change point (year)	K_t	P
AMP	1.71	Positive	4.03	−73.6 to 89.6 (mm/10a)	1989	−160	0.948
SDII	4.05	Positive**	0.05	−0.9 to 1.4 (mm/10a)	1992	−201	0.991
Rx1day	3.28	Positive**	0.54	−13.3 to 13.6 (mm/10a)	1995	−164	0.955
Rx5day	4.36	Positive**	1.23	−15.2 to 24.1 (mm/10a)	1992	−214	0.995
RX95p	3.54	Positive**	2.70	−76.2 to 73.3 (mm/10a)	1993	−164	0.955
RX99p	2.79	Positive**	0.96	−31.0 to 11.1 (mm/10a)	1995	−130	0.858
APD	2.09	Positive*	0.17	−5.0 to 12.5 (days/10a)	1989	−118	0.799
R10 mm	3.68	Positive**	0.16	−1.2 to 5.0 (days/10a)	1989	−216	0.995
R20 mm	4.17	Positive**	0.11	−1.1 to 3.5 (days/10a)	1989	−218	0.996
R50 mm	2.92	Positive**	0.02	−0.7 to 0.5 (days/10a)	1993	−138	0.889
CDD	3.47	Positive**	0.22	−8.3 to 3.5 (days/10a)	2003	−162	0.952
CWD	2.79	Positive**	0.03	−0.7 to 1.2 (days/10a)	2005	−132	0.866

*Significant at the 0.05 level.
**Significant at the 0.01 level.

1.23 mm/decade, respectively, based on their Sen's slope estimator. Meanwhile, the number of rain days with daily precipitation exceeding the 95th and 99th percentiles and related precipitation intensities have an increasing tendency during the past 37 years with a regional average of 2.70 and 0.96 mm/decade, respectively, based on the Sen's slope estimator. Moreover, the largest trend rate of extreme precipitation indices is R95pTOT, varying from −76.2 to 73.3 mm/decade, with a regional average of 2.70 mm/decade, indicating that Jinan is suffering a growing number of extreme precipitation events over its whole administrative region. On the other hand, both the CDD and CWD experienced statistically significant increasing trends at the 0.01 significance level, resulting in frequent drought and flooding disasters during the past few decades. Zhang *et al.* (2008) and Zhai *et al.* (2005) also indicated that the precipitation maxima increased but the rainy days decreased significantly in the lower Yellow River Basin. Thus, there is a dominant increasing trend for both the precipitation amount and intensity, which is consistent with the intensification of the hydrological cycle in Jinan City.

According to the result of the Pettitt test, the change points of most indices appear approximately in 1990, but for the CDD and CWD, it is mainly around 2005. However, since every P value is larger than 0.05, all of these change points are not significant at 95% confidence level, indicating that the change points for the 12 indices are insignificant.

To further investigate the characteristics of the spatiotemporal variation in extreme precipitation over Jinan City during the past 37 years, a spatial distribution for the M–K trends of the 12 extreme precipitation indices per decade is illustrated in Figure 6.

According to Figure 6(a), most of the northern plain and east mountainous areas show a significant increasing trend at a maximum rate of 89.6 mm/decade for AMP, while the southwest area experiences a decreasing trend at a minimum rate of −73.6 mm/decade (insignificant), with a regional average of 4.03 mm/decade overall. The APD shows a significant increasing trend mainly in the north central and eastern mountainous area in Jinan City, while the main urban area experiences a decreasing trend, but is not significant (Figure 6(g)). Moreover, the SDII shows a significant increasing trend in northern and eastern Jinan City, especially in the north central area (Figure 6(b)). Meanwhile, it decreases significantly in the southwestern mountainous area, with a minimum value of −0.9 mm/(day·decade). However, Wang *et al.* (2013) and Xu *et al.* (2007) indicated that AMP and APD of the downstream region of the Yellow River Basin showed a decreasing trend. The differences are probably caused by the rain island effect and tropical island effect induced by continuous urban expansion during the booming stages of industrialization and urbanization in urban areas.

From Figure 6(c), the Rx1day shows a significant increasing trend in northern and eastern Jinan City (urban area included), where the AMP is originally small, while the southwestern mountainous area experiences a significant decreasing trend, where the AMP is relatively large, varying from −13.3 to 13.6 mm/decade, which is the opposite of the spatial distribution of Rx1day. RX95p and RX99p show the same spatiotemporal variation characteristics as Rx1day (Figure 6(e) and 6(f)). Rx5day shows a significant increasing trend, mainly in north central and eastern Jinan City, while the southwestern mountainous area experiences a decreasing trend, where the AMP is relatively large, varying from −15.2 to 24.1 mm/decade (Figure 6(d)).

Similarly, R10 mm and R20 mm show the same spatiotemporal variation characteristics as the AMP (Figure 6(h) and 6(i)), but varies greatly with R50 mm. Specifically, R50 mm experiences a significant decreasing trend in the southwestern mountainous area, but increases in part of the northern plain area (Figure 6(j)). In that case, the increasing AMP in the north plain and east mountainous area mainly results from increasing light to moderate rainfall rather than heavy rain or rainstorms, while the decreasing AMP in the southwestern mountainous area is the combined result of decreasing light to heavy rain there.

As shown in Figure 6(k) and 6(l), CWD have no significant change overall, while CDD show a significant decreasing trend mainly in the urban area. It is worth mentioning that several extreme precipitation indices, including Rx1day, Rx5day, and R50 mm, show a concentration trend in the middle part of Jinan City, which indicates that the urban area is more likely to encounter an aggregation of rainfall events with high intensities and short durations than suburban areas of similar latitudes, leading to a higher risk of floods in the urban area, which is likely to increase the uncertainty of water supply there and hence trigger new challenges for water resource management

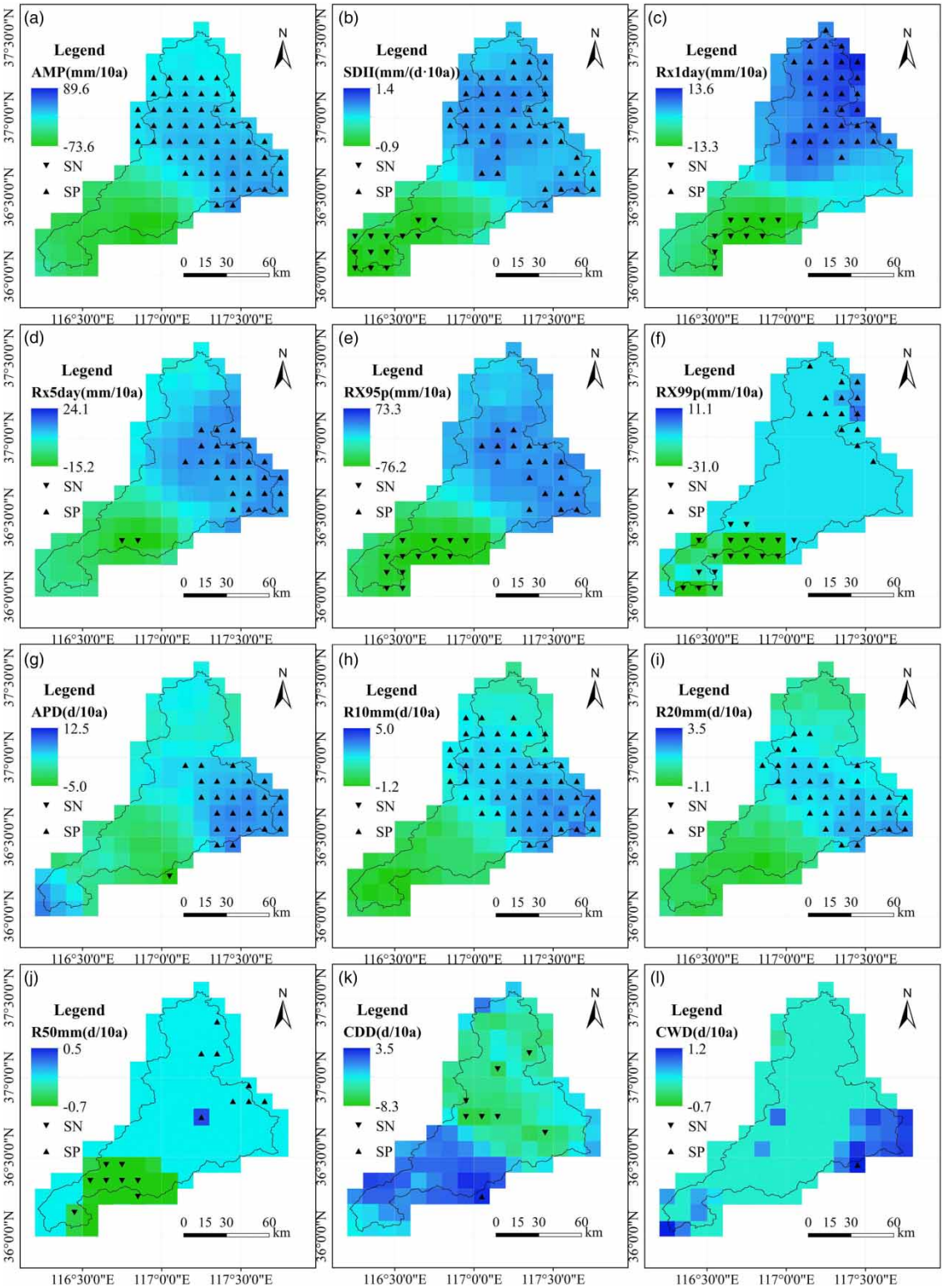

Figure 6 | Spatial distribution for the M–K trends of the 12 extreme precipitation indices per decade from 1979 to 2015 in Jinan City (SP means significant positive and SN means significant negative at the 95% confidence level in the legend). The gray line represents the boundary of the main urban area in Jinan City.

under the influence of climate change and human activities, such as the increasing water demand on account of the industry's rapid development and swift population growth. Zhang *et al.* (2014) also found that the lower Yellow River Basin may encounter a higher risk of flood and drought disasters due to the intensifying precipitation intensity, which is just coincident with the current conclusions.

CONCLUSIONS

In this paper, the spatiotemporal variation characteristics of the precipitation in Jinan City during 1979–2015 were investigated using the M–K trend test and other relative analysis methods. From the analysis in this study, some interesting conclusions have been drawn, as follows:

1. The spatial distribution of the AMP in Jinan City shows a gradient decrease from the southern mountainous area to the northern plain area, which varies greatly with local topography. It is highest in the mountainous area and lowest in the plain area, showing a rough positive correlation with local elevation. Since the mountainous area is immediately adjacent to the downtown area, the high AMP there may induce frequent flashflood disasters in the urban area.
2. The AMP in Jinan City has been increasing in volatility during 1979–2015, and there are significant interdecadal and interannual variations in precipitation amounts. The wet season precipitation in urban and plain areas experienced a marked increase overall during the past 37 years, while it decreased obviously in the mountainous area. In addition, the dry season precipitation in the whole city has been progressively increasing with a small trend. Therefore, the steadily increasing trend in the wet season plays a dominant role in the trends of overall annual precipitation.
3. Compared with other seasonal precipitation in the whole city, summer precipitation has the largest proportions, accounting for more than 60% of the total annual precipitation. The spring and autumn precipitation for the whole city, is approximately 15% of the total AMP, while the winter precipitation is the lowest. In addition, the heaviest summer precipitation occurs in the mountainous area, especially for the southern part of the downtown area. Affected by topography, the rainstorm-generated runoff often flows downwards along the channels and valleys, making the north–south traffic artery the main flood canal towards the urban area, resulting in the drastic amplification of urban rainfall floods.
4. The spatial distribution of most indices shows a gradual increasing trend from the northern plain area to the southern mountainous area, while the distribution of CDD shows the opposite tendency. The urban area is more likely to encounter an aggregation of rainfall events with high intensities and short durations than suburban areas of similar latitudes. The APD and CWD are likely concentrated at the southwestern and east mountainous area where the AMP in those areas is not so large, indicating that less extreme precipitation occurred in those areas.
5. As for the spatiotemporal variation trends of precipitation-related indices, most of them have roughly the similar characteristics as AMP, i.e., decreased in the southwestern region but increased in the eastern mountainous area and north plain area. In addition, Rx1day shows a significant increasing trend in the main urban area at a rate of 3.1 to 8.6 mm/decade, leading to a higher risk of flash flood there. Generally speaking, the majority of precipitation-related indices exhibit an increasing trend overall at the 1% significance level as a whole. Since both the R50 mm and CDD show significant positive trends, it is suggested that both extreme rainstorms and droughts in Jinan City tend to be more frequent.

ACKNOWLEDGEMENTS

This study was supported by the research project from the Natural Science Foundation of China (No. 51579007). The authors acknowledge the Institute of Tibetan Plateau Research in the Chinese Academy of Sciences for providing a precipitation dataset with high resolution.

REFERENCES

Bonsal, B. R., Zhang, X., Vincent, L. A. & Hogg, W. D. 2001 Characteristics of daily and extreme temperatures over Canada. *Journal of Climate* **14** (9), 1959–1976.

Chen, Y., Yang, K., He, J., Qin, J., Shi, J., Du, J. & He, Q. 2011 Improving land surface temperature modeling for dry land of China. *Journal of Geophysical Research Atmospheres* **116** (20), 1–15.

Cui, B., Wang, C., Tao, W. & You, Z. 2009 River channel network design for drought and flood control: a case study of Xiaoqinghe River basin, Jinan City, China. *Journal of Environmental Management* **90** (11), 3675–3686.

Esteban-Parra, M. J., Rodrigo, F. S. & Castro-Diez, Y. 1998 Spatial and temporal patterns of precipitation in Spain for the period 1880–1992. *International Journal of Climatology* **18** (14), 1557–1574.

Gilbert, R. O. 1987 *Statistical Methods for Environmental Pollution Monitoring*. John Wiley & Sons, New York.

Hansen, J., Sato, M., Hearty, P., Ruedy, R., Kelley, M., Masson-Delmotte, V., Russell, G., Tselioudis, G., Cao, J., Rignot, E., Velicogna, I., Tormey, B., Donovan, B., Kandiano, E., Von Schuckmann, K., Kharecha, P., Legrande, A. N. & Bauer, M. 2016 Ice melt, sea level rise and superstorms: evidence from paleoclimate data, climate modeling, and modern observations that 2°C global warming could be dangerous. *Atmospheric Chemistry and Physics* **16** (6), 3761–3812.

IPCC 2014 Summary for policymakers. In: *Climate Change 2014: Mitigation of Climate Change. Contribution of Working Group III to the Fifth Assessment Report of the Intergovernmental Panel on Climate Change* (O. Edenhofer, R. Pichs-Madruga, Y. Sokona, E. Farahani, S. Kadner, K. Seyboth, A. Adler, I. Baum, S. Brunner, P. Eickemeier, B. Kriemann, J. Savolainen, S. Schlömer, C. von Stechow, T. Zwickel & J. C. Minx, eds). Cambridge University Press, Cambridge, UK and New York, USA.

Jauregui, E. & Romales, E. 1996 Urban effects on convective precipitation in Mexico City. *Atmospheric Environment* **30** (20), 3383–3389.

Jianting, C. H. U., Jun, X. I. A., Chongyu, X. U., Lu, L. I. & Zhonggen, W. 2010 Spatial and temporal variability of daily precipitation in Haihe River basin, 1958–2007. *Journal of Geographical Sciences* **20** (2), 248–260.

Jie, H. & Kun, Y. 2011 China Meteorological Forcing Dataset. Cold and Arid Regions Science Data Center at Lanzhou. [online] http://dx.doi.org/10.3972/westdc.002.2014.db.

Kendall, M. G. 1975 *Rank Correlation Methods*. Griffin, London, UK.

Liu, Q., Yang, Z. & Cui, B. 2008 Spatial and temporal variability of annual precipitation during 1961–2006 in Yellow River Basin, China. *Journal of Hydrology* **361** (3), 330–338.

Liu, W., Zhang, M., Wang, S., Wang, B., Li, F. & Che, Y. 2013 Changes in precipitation extremes over Shaanxi Province, northwestern China, during 1960–2011. *Quaternary International* **313–314**, 118–129.

Madsen, H., Lawrence, D., Lang, M., Martinkova, M. & Kjeldsen, T. R. 2014 Review of trend analysis and climate change projections of extreme precipitation and floods in Europe. *Journal of Hydrology* **519** (PD), 3634–3650. [online] http://dx.doi.org/10.1016/j.jhydrol.2014.11.003.

Mann, H. B. 1945 Nonparametric tests against trend. *Econometrica: Journal of the Econometric Society* **13**, 245–259.

Panthi, J., Dahal, P., Shrestha, M. L., Aryal, S., Krakauer, N. Y., Pradhanang, S. M., Lakhankar, T., Jha, A. K., Sharma, M. & Karki, R. 2015 Spatial and temporal variability of rainfall in the Gandaki River Basin of Nepal Himalaya. *Climate* **3** (1), 210–226.

Pettitt, A. N. 1979 A non-parametric approach to the change-point problem. *Applied Statistics* **28**, 126–135.

Sen, P. K. 1968 Estimates of the regression coefficient based on Kendall's tau. *Journal of the American Statistical Association* **63** (324), 1379–1389. [online] http://www.jstor.org/stable/2285891.

Sillmann, J., Kharin, V. V., Zhang, X., Zwiers, F. W. & Bronaugh, D. 2013 Climate extremes indices in the CMIP5 multimodel ensemble: part 1. Model evaluation in the present climate. *Journal of Geophysical Research: Atmospheres* **118** (4), 1716–1733.

Tang, Z., Wang, Z., Zheng, C. & Fang, J. 2006 Biodiversity in China's mountains. *Frontiers in Ecology and the Environment* **4** (7), 347–352.

Wang, R. & Li, C. 2016 Spatiotemporal analysis of precipitation trends during 1961–2010 in Hubei province, central China. *Theoretical and Applied Climatology* **124** (1–2), 385–399.

Wang, W., Shao, Q., Yang, T. & Sun, C. Z. Á. F. 2013 Changes in daily temperature and precipitation extremes in the Yellow River Basin, China. *Stochastic Environmental Research and Risk Assessment* **27**, 401–421.

Xu, Z. X. & Chu, Q. 2015 Climatological features and trends of extreme precipitation during 1979–2012 in Beijing, China. *Proceedings of IAHS* **369**, 97–102.

Xu, C., Widén, E. & Halldin, S. 2005 Modelling hydrological consequences of climate change – progress and challenges. *Advances in Atmospheric Sciences* **22** (6), 789–797.

Xu, Z. X., Li, J. Y. & Liu, C. M. 2007 Long-term trend analysis for major climate variables in the Yellow River basin. *Hydrological Processes* **21**, 1935–1948.

Xu, Y., Xu, J., Ding, J., Chen, Y., Yin, Y. & Zhang, X. 2010 Impacts of urbanization on hydrology in the Yangtze River Delta, China. *Water Science and Technology* **62** (6), 1221–1229.

Zhai, P., Zhang, X., Wan, H. & Pan, X. 2005 Trends in total precipitation and frequency of daily precipitation extremes over China. *Journal of Climate* **18**, 1096–1108.

Zhang, Q., Xu, C., Zhang, Z. & David, Y. 2008 Spatial and temporal variability of precipitation maxima during 1960–2005 in the Yangtze River basin and possible association with large-scale circulation. *Journal of Hydrology* **353**, 215–227.

Zhang, Q., Xu, C., Zhang, Z., Chen, Y. D. & Liu, C. 2009 Spatial and temporal variability of precipitation over China, 1951–2005. *Theoretical and Applied Climatology* **95** (1–2), 53–68.

Zhang, Q., Singh, V. P., Peng, J., David, Y. & Li, J. 2012 Spatial–temporal changes of precipitation structure across the Pearl River basin, China. *Journal of Hydrology* **440–441**, 113–122. [online] http://dx.doi.org/10.1016/j.jhydrol.2012.03.037.

Zhang, Q., Peng, J., Singh, V. P., Li, J. & Chen, Y. D. 2014 Spatio-temporal variations of precipitation in arid and semiarid regions of China: the Yellow River basin as a case study. *Global and Planetary Change* **114**, 38–49.

First received 11 January 2017; accepted in revised form 12 October 2017. Available online 11 November 2017